applied sciences

MDPI

Article

The Quest for Industrially and Environmentally Efficient Nanobubble Engineering: Electric-Field versus Mechanical Generation Approaches

Niall J. English

School of Chemical & Bioprocess Engineering, University College Dublin, Belfield, D04 V1W8 Dublin, Ireland; niall.english@ucd.ie

Abstract: Nanobubbles (NBs) are gaseous domains at the nanoscale that can exist in bulk liquid or on solid surfaces. They are noteworthy for their high potential for real-world applications and their long (meta)stability. "Platform-wide" applications abound in medicine, wastewater treatment, hetero-coagulation, boundary-slip control in microfluidics, and nanoscopic cleaning. Here, we compare and contrast the industrial NB-generation performance of various types of commercial NB generators in both water-flow and submerged-in-water settings—in essence, comparing electric-field NB-generation approaches versus mechanical ones—finding that the former embodiments are superior from a variety of perspectives. It was found that the electric-field approach for NB generation surpasses traditional mechanical approaches for clean-water NB generation, especially when considering the energy running cost. In particular, more passive electric-field approaches are very operationally attractive for NB generation, where water and gas flow can be handled at little to no cost to the end operator, and/or submersible NB generators can be deployed, allowing for the use of photovoltaic approaches (with backup batteries for night-time and "low-sun" scenarios and air-/CO_2-pumping paraphernalia).

Keywords: nanobubbles; energy; sustainability

Citation: English, N.J. The Quest for Industrially and Environmentally Efficient Nanobubble Engineering: Electric-Field versus Mechanical Generation Approaches. *Appl. Sci.* **2024**, *14*, 7636. https://doi.org/10.3390/app14177636

Academic Editor: Andrea L. Rizzo

Received: 10 August 2024
Revised: 24 August 2024
Accepted: 26 August 2024
Published: 29 August 2024

1. Introduction

Limited solubility of gases in many liquids (typically below Henry's-Law levels), e.g., gases in water, such as oxygen and especially hydrogen, is a fundamental challenge. In ecosystems and the environment, lack of dissolved oxygen (DO) is a major reason for fish kills and water bodies being blighted by algal blooms, in addition to, sometimes, a lack of effectiveness of activated-sludge processes in water treatment or poorer-than-hoped results in irrigation. Nanobubbles (NBs) are gaseous domains on the nanoscale, existing on solid surfaces or in bulk liquid—noted for their long-time (meta)stability and high potential for real-world applications [1–3], e.g., nanoscopic cleaning [4], boundary-slip control in microfluidics [5], wastewater treatment [6], hetero-coagulation [7], and medical applications [8]. While NBs on surfaces have been observed, NBs in the bulk have been studied less [2,3]. It is speculated that NBs' long-lived presence arises from negative-charge build-up at the bubble/liquid interface, with the surface having strong electron affinity [9]. Generated properly, nanobubbles offer a chance, promisingly, to overcome fundamental gas-in-liquid solubility "bottlenecks".

The concept of nanobubbles versus traditional, coarser bubbles, is illustrated on the top right of Figure 1—with the latter subject to buoyancy phenomena, while NBs are relatively impervious to rising—in essence, subverting Stokes' Law of bubble rising [2,3]. In liquids, bubbles have internal equilibrium pressures at least that of the external environment. Each bubble is surrounded by an interface that possesses different properties to that of the bulk solution. In any event, microbubbles are not stable for long periods (~minutes), rising slowly and indirectly to the surface, but smaller ones (≈<20 μm diameter) will shrink to

form more effective and stable NBs [3]. Only these tiny bubbles (<1 µm diameter) are stable for significant periods in suspension [1,2]. The surface area of a volume of bubbles is in inverse proportion to the bubble diameter. Thus, for the same volume of the bubble, their surface area increases proportionally to the reduction in bubble diameter, meaning that NBs have an excellent area-to-volume ratio, as is evident in the top right of Figure 1. In such a way, we can enhance greatly gas–liquid mass transfer—of which we shall consider further anon (vide infra). Naturally, if NBs are generated well—indeed, the art of "nanobubble engineering", as it were—the stability of NBs, together with their high surface area per volume, leads to important and useful applications.

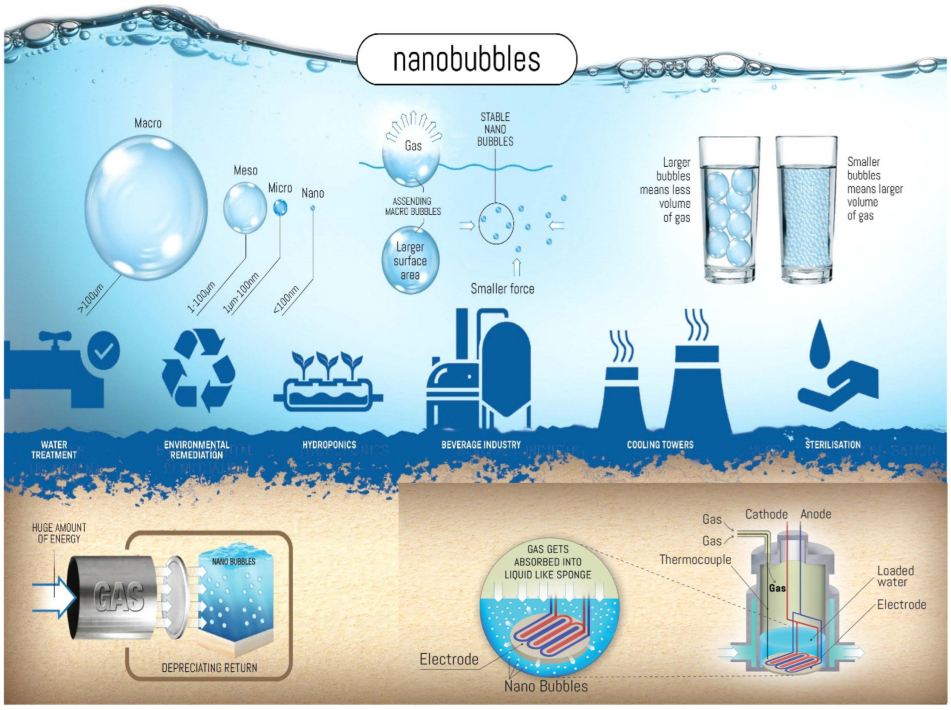

Figure 1. Graphical summary of the scope of non-equilibrium nano-dispersed fluids, with the bottom-right inset section showing the electrostriction concept. (Image credit: Jon Tallon).

In terms of the status quo (ante) vis-à-vis industrial NB generation, the bottom left of Figure 1 depicts the "forced-convection" approach, whereby traditional (mechanical) generation methods mainly rely on hydrodynamic, acoustic, particle, and optical cavitation, in tandem with injecting pressurised gases through a tubular ceramic membrane lined by nano-pores—which, inevitably, just get biofouled in short order. These NB-generation processes raise issues such as, inter alia, high energy consumption, non-flexibility, and complexity. In stark contrast, on the bottom right, we see the disruptive electric-field invention, whereby the application of static electric fields via sheathed electrodes to water–gas systems promotes the instant and low-energy formation and build-up of ultra-dense gas nanobubbles inside the liquid phase, by enhancing metastable gas solubility through electrostrictive action [10,11]. This endows these "thick-skinned" NBs with unique environmental and industrial applications [12,13], realising nano-porous liquids (NPLs) as a new class of 'designer' green solvents. Nanobubbles, with greater mass density than mechanical-generation approaches, generated properly by canny and effective electric-field nanobubble engineering [14–17], offer a chance, promisingly, to overcome fundamental gas-in-liquid solubility "bottlenecks"—often with important environmental benefits [18,19].

Following the discovery and invention of both surface-electrostatic nanobubble and nanodroplet generation and stabilisation via application of external electric fields to gas–liquid systems (at arbitrary gas pressures), with the dramatic result of massively increased gas uptake into the liquid in NB form [10,11], in the present article, we compare this

to traditional mechanical-generation approaches. The de facto long-lived gas-solubility enhancement ranges up to 2.5-fold for oxygen to 30-fold for methane vis-à-vis respective Henry's-Law values for gas solubility. Indeed, molecular-dynamics simulations reveal that the origin of nanobubbles' movement lies in dielectrophoresis, with their resultant 'thick skin' of a quasi-liquid layer and mutual dipolar and electrostatic repulsion affording a good degree of mutual NB stabilisation (often with half-lives of many months) [11]—and with sustained lifetimes at high temperatures. Intriguingly, we can also create nanodroplets—at will—via the application of external electric fields [14] and other methods [20]; although, the present study is focused on NB generation per se.

In view of the need to explore new nanobubble-engineering approaches, and gauge comparative efficiencies of traditional, mechanical-centric versus electric-field approaches, the present study compares and contrasts the performance of commercial bulk-nanobubble generators of various types from various perspectives—including, inter alia, the energy efficiency of NB generation, absolute NB populations, and mass density of NBs, as well as the proportion of bulk NBs compared to the entire bubble-size population.

2. Brief Review of Nanobubble-Generation Approaches

Many researchers and companies have focused on inventing, developing, and scaling up various techniques to generate nanobubbles in large concentrations—preferably with an adjustable size distribution based on the intended final application—and, often, scaling up to industrial performance, if possible.

2.1. Porous-Medium Membrane

The first main mechanical NB-generation approach is predicated on fluid flow through porous media [21–24]. Pressurised injection gas is fed through the medium membrane to make bubbles (especially in water). By reducing the sizes of pores in the medium, metastable-bubble sizes of less than 1 μm can be achieved. For example, the Anzai Kantetsu, Acniti, and Molaear companies all use systems in which a pressurised gas is injected into a passage and then a fine-carbon-based porous medium with pore diameters of several nm to several tens nm. The porous medium, which is positioned horizontally or tilted downwards, should obey a defined shortest-to-longest distance ratio between the medium and the flow passage. The fluid flowrate and gas pressure are other important factors in this system.

While most methods involve injecting the gas through a fine porous medium to create nanobubbles, some propose passing the liquid–gas mixture through a filter or porous medium to reduce the size of the bubbles and only permit bubbles smaller than a threshold to pass through. For instance, Sang is offering a system that uses a Venturi section to draw raw water and water flow to create a relative pressure that allows gas to be drawn in [24]. After being pressurised, the gas–water mixture goes through three stages of filtering. In the initial stage, large bubble sizes are filtered together with foreign particles using a sponge, non-woven filter, or ceramic porous media. The bubbles are finer in the second stage, which has beads layered on top of each other, and the bubbles are filtered in the third stage, which shares the same structural design as the first stage, to produce bubbles with nanoscale order and nearly identical sizes.

2.2. Pressure Difference

A mechanical crack between two points can cause a fluid to flow; the size of the crack and other fluid properties determine how much of the flow is turbid and other parameters. The mechanical pressure difference between two locations in the flow of a liquid–gas mixture is one of the fundamentals used in some methods for the generation of nanobubbles. Toshihiko disclosed a pump drawing in gas and water, pressurising the gas–water mixture inside a tank [25]. A pressure-regulator valve that controls the mixture's pressure in the place of generation connects the pressurised mixture to the location where nanobubbles are produced. There is an orifice at the system's discharge section that aids

in regulating pressure where nanobubbles are generated. Controlling the ratio of P_2/P_1, where P_2 is the pressure before the orifice and P_1 is the mixture pressure before the pressure-regulating valve, is essential for this system to produce nanobubbles of the right size and population. Pressure differences may also be achieved by the judicious use of static mixers. The cavitation principle of nanobubble generation—featuring in a number of industrial-generator designs—also exploits the creation of a pressure difference: Shuhei and Hitomi disclosed a pressure-differential cavitation system based primarily on a suction pump that intakes water and gas via negative pressure, mixes the mixture, and makes foam-like bubbles, which enter a flat area and create swirl-like cavitation to make the bubbles finer to achieve nano-sized bubbles [26].

2.3. Shear Stress

A widely used method makes use of shear stress and friction forces to induce bubbles to break into smaller ones progressively, to finally reach fine- and nano-sized bubbles. Flow-rotational approaches are also used in some submersible NB-generator designs, predicated on such frictional forces, and this is used in some Moleaer and Acniti submersible designs. Ho et al. outlined a gas–water mixture flowing through a chamber containing a rotating shaft with different protruding units [27,28]. Smaller bubbles may result from these units' ability to rub the gas–water mixture and its circumferential surface. The system consists of multiple steps that produce microbubbles in the initial stages and then reduce them to produce nanobubbles, optionally with boundary-layer mixing by passing a gas–water mixture through a long hose.

The Acniti microStar "hammermill-rotation" submersible NB generator, together with the submersible-unit design of Moleaer featuring a "rotating-shaft" (with an associated porous membrane for bubble-size reduction towards the nanoscale range) [29], feature this general concept of rotational-swirl flow arrangements predicated on the general concept of shear-stress/frictional-induced progressive bubble-size reduction.

2.4. External Electric Field

An externally applied static electric field can be used on gas–water systems to induce the formation of nanobubbles and/or nanodroplets [10,11]. The presence of this external electric field in proximity to a volume of liquid containing a medium facilitates the generation of nanobubbles or nanodroplets via electrostrictive capture of a sub-population of nanobubbles (or -droplets) from the outer periphery of upstream/incipient population of macro-, meso-, or microbubbles. This external-field-induced modus operandi is effective at transforming a large portion of either upward-rising macro- and/or mesobubbles, or vertically or horizontally flowing bubbles, in ultra-dense and long-lived NBs. This energy-efficient, "sheathed-electrode" method, bereft of moving parts, lends itself well to low-maintenance and solar-powered operations for off-grid work [14,18,19]. The approach has been used for gasification of water for both flow- and submersible-based types of NB generators [30–33], as well as for petroleum aeration and thermodynamic-cycle efficiency (ICEs) [34].

3. Materials and Methods

In order to compare various types of commercially available NB-generation approaches for NB generation in water, five commercial liquid-flow-based NB generators were used in the present study, as well as two commercial submersible NB generators—submerged either partly or fully in water. These are detailed in Table 1, with label numbers (1 to 7); in addition, the AquaB flow units are appended by "V" or "C" to denote Venturi- or compressor-fed for the upstream gas-input section. These units were not run for more than a few hours, given that the current study is not focussed on longer-term use, biofouling, or maintenance issues: rather, the focus is on absolute and comparative NB-generation efficiencies.

Table 1. List of smaller-scale commercial water-flow and submersible NB generators studied.

Type/Model	Water Flowrate (Litres per Minute, 'lpm')/Operation Remarks	Ref.
1: Flow: Moleaer Kingfisher	40–160 lpm; in-house compressor and water pump	[34]
2: Flow: Acniti Turbiti 727	30–80 lpm; Venturi with no supplied water pump	[35]
3 (V, C): Flow: AquaB In-line Tubular Pipe	20–120 lpm; Venturi or compressor; supplied water pump	[36]
4 (V, C): Flow: AquaB Radial Vortex	120–260 lpm; Venturi or compressor, water pump supplied	[36]
5: Flow: Anzai Porous Membrane	~10 lpm; pressurised air/O_2 source; watch back pressure	[37]
6: Sub: Acniti microStar FS-400	Air/ozone/CO_2-flow: 5–50 lpm (STP); keep motor above water line	[38]
7: Sub: AquaB Small-Scale Sub	Air/ozone/CO_2-flow: 3–45 lpm (STP); fully submerged	[36]

It was decided to carry out aeration with the five flow generators (1 to 5), whilst air was supplied to the submersible units (6 and 7); neither ozone nor CO_2 was considered for the submersible units in the present study. Although the "hammermill-rotation" Acniti microStar (6) is submerged in water, the associated 400 W motor needs to be kept above the water line, as this is not water proof.

Of the five flow units, the Anzai one (5) requires more of a pre-pressurised gas source—air or oxygen, at typically up to 4.5–5 bar g regulator/delivery pressure—although, the best result for boosting DO requires the use of essentially pure O_2 for efficient flow through the micro-nano-porous-medium membrane. To be fair in comparisons to other water-flow NB generators in the present study (1 to 4), we only discuss the use of air.

For the Moleaer Kingfisher (1) and Acniti Turbiti (2), on the one hand, internal water pumps and compressed air (with partial internal ozone mixing) and, on the other, Venturi air-draw approaches are leveraged, respectively. This adds substantially to overall product complexity (including maintenance considerations) and operational energy requirements by way of larger pressure drops across the units. The energy consumption will be considered later. The AquaB flow units—both the in-line tubular pipe-style model (3) and the larger-flowrate vertically mounted radial-vortex unit (4)—may operate either with lower-pressure-drop coarser-bubble Venturi sections (V) or else with compressors or gas-cylinder feeds (C). The "default" of using a Venturi section for ambient-air capture works comparatively well vis-à-vis compressor or cylinder gas feed for, e.g., nano-aeration, when considering the level of Venturi-driven NB production, given the pressure-drop equivalence of Venturi use against air-compressor energy budgeting (vide infra).

In terms of the water source, filtered tap-water was used: a three-stage water reverse-osmosis filter from AquaClear Ltd. was used for Dublin-area tap-water, and filtering was carried out until the derived count rate in a Malvern Zetasizer Pro (from Malvern Panalytical) was just below the 100 k.c.p.s. threshold, so as to minimise the level of (light-scattering) impurities. This is important for reproducibility and to allow reasonable levels of statistical error to be found. It was found that there was no NB detection found in background water samples without being passed through water-flow-based NB generators or used in conjunction with submersible units.

For Dynamic Light Scattering (DLS), a Malvern Nanosight Pro was also used in the case of the flow units for comparison purposes, to use the NTA particle/bubble-tracking approach as arguably a more consistent bubble-counting/detection metric than Zetasizer Pro multi-angle DLS (MA-DLS), although nanobubble populations can be truncated for detection purposes in some cases below 35 nm, and the lower concentration detection

limits for both types of Malvern instrument were on the order of around 10^6 NBs per mL for the relatively clean, filtered tap-water (to somewhat below a workable and pragmatic 100 k.c.p.s. "light-scattering quality threshold") [39].

The NB populations were assessed via laser scattering on a time-resolved basis after running the flow generators at around their mid-range water flowrate for 4 min: there would typically have been a few passages of the water through the units at that stage vis-à-vis their respective flow residence times. Air flow was set to be about 1:15 in STP-litres versus the water flowrate; when using external/internal air compressors, the discharge pressure was typically ~3.5–4 bar g. The power draw was monitored, and external water-pumping costs were added in to the "power-reckoning" budget (with water-pumping power costs higher for optional "Venturi-draw" operation in some cases, albeit displacing air-compressor costs). For submersible units, the power draw was also recorded in 20 L of water and NB populations sampled after 20 min and was tracked thereafter. The pH was also tracked, as well as DO, with an optical Mettler Toledo probe.

These NB-generation performance figures are quoted in Section 4 below for potential off-grid deployment of the AquaB tubular-flow unit where explicit local water and air pumping is not possible (or simply not desired), albeit it must be borne in mind that the additional pressure drop is ultimately borne by the municipal mains water (or upstream water) provider, and would typically be equivalent to ~50–75 W of water-pumping power. Naturally, it is not desired to give the impression that the lower-energy, "Off-Grid" and low-power mode of the AquaB tubular unit, Venturi-mode operation is only ~4–8 W (whether solar-/battery-powered or not), as that would be completely misleading—although that is what the end-operator would actually incur assuming that they were not liable for additional charges on greater water-pumping costs—which may or may not be the case.

4. Results and Discussion

The DLS-determined NB populations taken directly after air-fed flow are provided below in Table 2. This was an average over three measurements, although Moleaer (1) and Anzai (5) did not register above the NB detection threshold in all cases; the number of asterisks beside the relevant population determine the number of times a NB population could actually be determined.

Table 2. NB populations ($\times 10^6$ NBs per mL) and power from air-fed water-flow operation; AquaB is in both Venturi and air-compressor modes. The number of asterisks shows the number of successful detections of nanobubbles out of three attempts. If there is only one measurement of three ("*"), an uncertainty cannot be measured, as, by definition, a standard deviation cannot be computed under the circumstance of only a single viable measurement.

Type/Model	Zetasizer Pro	Nanosight Pro	Power Draw (W)
1: Moleaer Kingfisher	4.82 *	3.26 *	1085
2: Acniti Turbiti 727	6.5 *** ± 2.9	4.1 ** ± 1.1	585
3V: AquaB In-line Tubular Pipe (Venturi)	43 *** ± 9	32 *** ± 5	280
3C: AquaB In-line Tubular Pipe (Air Comp.)	71 *** ± 11	42 *** ± 7	370
4V: AquaB Radial Vortex (Venturi)	88 *** ± 13	71 *** ± 8	570
4C: AquaB Radial Vortex (Air Comp.)	110 *** ± 18	94 *** ± 11	660
5: Anzai Porous Membrane	1.22 *	1.03 *	290

In the case of the AquaB radial-vortex approach operated in air-compressor mode (4C), similar results were obtained via independent-party measurements [40].

Of course, it is possible to run the in-line AquaB units (3) without a water pump at lower water flowrates, on the order of 8–15 lpm, characteristic of domestic or light industrial municipal tap-water supply at ~0.5 bar g delivery pressure. In that case, if one ignores the local water-pumping cost (that is now borne instead by the mains-water-providing utility, or the upstream water provider in general), and uses a Venturi arrangement (3V), the power draw borne by the end user operating the in-line AquaB NB generator is as little as ~4–8 W (i.e., in essence, the overhead of AC-to-DC conversion)—cf. Table 3.

Table 3. NB populations ($\times 10^6$ NBs per mL) and AC–DC electric power during AquaB "Off-Grid"/"low-power" air-fed water-flow operation at municipal water tap-driven operation of ~10 lpm water flowrate (~0.5 bar g discharge pressure) with Venturi air draw—type 3V. Electric-power water-pumping equivalent of water-flow pressure drop is estimated—which may or may not be borne by the end user of the NB generator. The number of asterisks shows the number of successful detections of nanobubbles out of three attempts.

Type/Model	Zetasizer Pro	Nanosight Pro	AC–DC (W)	Estd. Pressure-Drop Pump Power (W)
3V: AquaB In-line Tubular Pipe	13 *** ± 6	14 *** ± 3	6 ± 1.5	55 ± 5

It is clear that the greater level of internal flow turbulence inside the various NB generators promotes a greater level of macro- and mesobubble formation, as is evident from turbidity observations. In the case of AquaB electrostriction generators, this can also be seen, although to less effect, given that there appears to be a higher conversion of such larger bubbles into NB form (vide infra). It is also clear that there is a systematically higher population using the Zetasizer approach compared to Nanosight, with a greater level of uncertainty therein; the different light-scattering approaches render NTA of the Nanosight approach arguably more consistent and conservative, albeit with the 35 nm threshold in the case of NTA often underestimating the population—more particularly so for smaller AquaB NBs.

The typical NB diameters, when detected, were ~70–90 nm for AquaB (3 and 4), 75–95 nm for Anzai (5) and Acniti (2), and 80 to 105 nm for Moleaer (1). Coupled with higher AquaB NB populations, the slightly smaller size of the AqauB-generated NBs boosts oxygen-transfer efficiency with a superior surface-area-to-volume ratio (cf. Figure 1, top right, for a visual comparison of different bubble sizes in the sense of surface area to volume).

Greater internal flow path turbulence at higher water and air flowrates can also, in the case of AquaB flow units, boost the NB population in non-linear proportion to the water and air flows and the power incurred in the air and water flows (whether using Venturi or air-compressor modi operandi); the data in Table 2 are quoted for typical mid-range flowrates of each device. This arises from more efficient mesobubble formation upstream of the internal electrode arrangement for meso-to-nanobubble conversion. It can be seen from the superior AquaB NB populations that the use of an air compressor, if available, is often helpful if higher performance is desired vis-à-vis the energy input. However, in the case for flow through porous membranes in the non-AquaB examples, there is a non-linear relationship with pressure drop, which, unfortunately, hampers the energy efficiency of their NB production—and can, in time, lead to greater membrane biofouling (although the present study does not concern itself with the thorny issue of biofouling and ongoing operability issues) [41].

The estimated mass of oxygen in NBs is presented in Table 4, although this may be expected to be somewhat of an underestimate, as well as the overall mass created in the mid-range flowrate, and this latter parameter is then normalised per unit power, and the "low-power" mode of the AquaB in-line tubular NB generator is also presented (with the 'end user' either "paying"—or not—for the use of electric energy for pumping water which is roughly equivalent to the "mains-water-line" and "Venturi-on-unit" flow-pressure drops).

Table 4 shows clearly that the well-engineered flow turbulence of the AquaB radial-vortex flow layout, flowing about electrodes, is the most energy-efficient, in terms of producing one gram per minute of O_2 in NB form in its circa 200 lpm pumped water flow, or a deal more when using the air-compressor mode (as opposed to simply regularly dissolved oxygen—cf. Table 5).

Table 4. O_2-in-NB-form mass estimate (mg/L) and in mg/min, given the water flowrate, and normalised to mg/J. The number of asterisks shows the number of successful detections of nanobubbles out of three attempts.

Type/Model	O_2—NBs (mg/L)	O_2—NBs (mg/min)	O_2—NBs (mg/min/W)
1: Moleaer Kingfisher	0.15 *	21	0.019
2: Acniti Turbiti 727	0.2 ** ± 0.04	10 ± 3	0.017 ± 0.005
3V: AquaB In-line Tubular Pipe (Venturi)	2.15 *** ± 0.35	130 ± 25	0.46 ± 0.08
3C: AquaB In-line Tubular Pipe (Air Comp.)	2.85 *** ± 0.4	285 ± 40	0.77 ± 0.12
4V: AquaB Radial Vortex (Venturi)	5.45 *** ± 1.0	980 ± 140	1.72 ± 0.2
4C: AquaB Radial Vortex (Air Comp.)	7.2 *** ± 1.1	1730 ± 210	2.62 ± 0.29
5: Anzai Porous Membrane	0.08 *	2	0.007
3V: AquaB In-line (Off-Grid, incl. P-drop)	1.0 *** ± 0.2	10 ± 2	0.16 ± 0.016
3V: AquaB In-line (Off-Grid, excl. P-drop)	1.0 *** ± 0.2	10 ± 2	1.67 ± 0.16

Table 5. DO boost levels (mg/L) at mid-range water flowrates and normalised to power.

Type/Model	DO Boost (mg/L)	Overall DO Boost per Watt (mg/W)	Negative pH Shift
1: Moleaer Kingfisher	3.1 ± 0.2	0.4 ± 0.03	0.07 ± 0.01
2: Acniti Turbiti 727	3.4 ± 0.2	0.29 ± 0.025	0.08 ± 0.01
3V: AquaB In-line Tubular Pipe (Venturi)	3.6 ± 0.25	0.77 ± 0.06	0.13 ± 0.01
3C: AquaB In-line Tubular Pipe (Air Comp.)	4.3 ± 0.3	1.16 ± 0.1	0.16 ± 0.01
4V: AquaB Radial Vortex (Venturi)	4.5 ± 0.3	1.42 ± 0.12	0.21 ± 0.01
4C: AquaB Radial Vortex (Air Comp.)	5.2 ± 0.35	1.89 ± 0.14	0.24 ± 0.01
5: Anzai Porous Membrane	1.6 ± 0.1	0.14 ± 0.01	0.06 ± 0.01
3V: AquaB In-line (Off-Grid, incl. P-drop)	2.4 ± 0.2	0.4 ± 0.03	0.1 ± 0.012
3V: AquaB In-line (Off-Grid, excl. P-drop)	2.4 ± 0.2	4 ± 0.3	0.1 ± 0.012

The mass-density of AquaB NBs is thought to be on the order ~1.5–2 times that of mechanically produced NBs, bearing in mind the Laplace pressure of NBs: it would appear that electrostriction leads to a greater build-up of guest/gas molecules at the water–bubble interface [10]. Of course, overemphasis on the NB population per se (bearing in mind potential underestimates from Nanosight distance-detection diameter cut-off and/or potential spurious detection from the Zetasizer), or indeed the overall mass in NB form, and/or mass-density of the NBs themselves, can potentially distract the operator from considering other aspects that are also very important: chiefly, the presence of reactive oxygen species and the overall oxidative potential of the water (e.g., by way of Oxidative Reduction Potential) [19]. In many cases, it is arguable that NB-imparted oxidative effects [6,18,19], via hydroxyl radicals, for instance, are crucially important in securing the best outcomes form NBs. It has been shown that the de facto ROS population from the AquaB electric-field approach generates a significant level of ROS, using ORP and photoluminescence measurements [19], although this was less evident in the present study for mechanically generated NBs.

In terms of the level of boost in DO and pH shift arising from use of the flow-based NB generators, this is summarised in Table 5. It is important to note that DO probes do not measure directly the presence of NBs per se: rather, over time, the rate of NB release into the classically dissolved DO phase can lead to an indirect and rough assessment of the mass in NB form, bearing in mind the prevailing chemical and/or biological oxygen demands (which are low in the present heavily filtered municipal tap-water) [30]. Of course, there are more direct measurements of the mass concentration of the flow-generated nanophase in Table 4—which may underestimate more severely the lower levels of mechanically generated NBs' overall mass due to systematic underestimation measurement errors in headspace gas. Even so, bearing in mind this important note and qualifying caveat, the greater NB mass and energy efficiency in NB generation via the electric-field approach is noted, which passes ANOVA analysis at the 99% confidence level. The greater negative pH shift is also noted for the electric-field approach (owing, in part, to greater levels of nano-carbonation) [10].

Once more, a note of caution is imparted to the reader that the "headline measurement" of a boost in DO, even if expressed in terms of per-Watt power efficiency, is further "clouded" by the precise number of residence-time recirculations, etc., in flow units from different manufacturers and different power draws and levels of internal turbulence and macrobubble dissipation prior to passage to an electric-field or porous-membrane chamber. Too often, the almost sole focus of actual or would-be NB-generator operators is on DO boost per se (or traditionally dissolved gas in general)—which does not capture NB production levels (unless the NBs destabilise within seconds to minutes after their birth) and does not consider the actual population or mass of NBs (and, even more subtly—and yet perhaps even more importantly—ORP/ROS, and wider oxidative benefits). Overly overt and prominent consideration of DO boost (or increase in any dissolved gas level), in the absence of considering other more subtle (and sometimes more difficult-to-measure) metrics (like ORP, although relatively straightforward to measure) [19] may shift the performance focus of NB generators instead to general hydrodynamic-/eddy-current-driven oxygen/CO_2/gas mixing and transfer into the classically dissolved phase (i.e., Henry's Law of individually solvated guest molecules which electrical resistance and/or optical probes are trained to detect to the detriment of detecting NBs, ipso facto). Given that the focus of NB generators ought, logically, to be on NB generation per se, as opposed to producing larger bubbles in the bubble-size distribution (with their faster Stokes'-Law dissipation dynamics from the liquid to atmospheric discharge, or at least phase segregation into a headspace above the liquid in a scenario not open to atmosphere), it is not inappropriate to consider the portion of NB mass created, as opposed to those of larger bubbles. We may do this by comparing Tables 4 and 5—cf. Table 6; here, we also estimate the approximate percentage of conversion into NBs as a proportion of incoming gas (O_2-in-air) flow, as well as the portion of classically dissolved versus "nano-dissolved" oxygen.

It can be seen that the electrostriction NB generators lead to approximately a quarter of the incoming oxygen in the air feed, whether via Venturi or air-compressor, converting into NBs, with that proportion rising slightly with greater turbulence and concomitant upstream mesobubble generation. Even though there may well be a more severe underestimate of the level of mass of O_2 in NB form vis-à-vis the mechanical NB generators (1, 2, and 5), a level of mass conversion of no more than 1–2% into NBs—at best—is not ideal. Although a thorough analysis of turbidity has not been carried out in the present study, the greater level of cloudy turbidity observed for the just-generated waters emanating from the mechanical "NB" generators is an obvious visual clue of a larger portion of visual-range meso- and microbubbles, which is confirmed in the estimates of Table 6 of no more than ~5–6% of the total dissolved O_2 mass being in NB form in those cases.

The Stokes' Law escape of larger meso- and microbubbles over minutes to hours, as witnessed visually and anecdotally by less "milkiness", suggests that one should focus instead, and more usefully, on the time-resolved dissipation of NB populations per se via laser-light scattering—given that the present study is not concerned with Stokes' Law

dissipation of such larger bubbles over such short timescales. By carrying out $\exp(-t/\tau)$ fits to time-resolved measurements of NB populations over hours to days, we estimate the negative-exponential NB dissipation "relaxation times", τ, as depicted in Table 7.

Table 6. Oxygen NB mass as a percentage of total dissolved O_2 (i.e., DO boost + NB) and as % of incoming gas.

Type/Model	% of Total Dissolved O_2	% of Incoming O_2
1: Moleaer Kingfisher	4.6	0.6
2: Acniti Turbiti 727	5.6	0.8
3V: AquaB In-line Tubular Pipe (Venturi)	37	23
3C: AquaB In-line Tubular Pipe (Air Comp.)	40	28
4V: AquaB Radial Vortex (Venturi)	55	30
4C: AquaB Radial Vortex (Air Comp.)	58	34
5: Anzai Porous Membrane	4.8	0.9
3V: AquaB In-line (Off-Grid, incl. P-drop)	29	21
3V: AquaB In-line (Off-Grid, excl. P-drop)	29	21

Table 7. Negative exponential decay relaxation times, τ (days), on the NB populations for the water-flow NB generators.

Type/Model	τ
1: Moleaer Kingfisher	1.4 ± 0.25
2: Acniti Turbiti 727	1.6 ± 0.28
3V: AquaB In-line Tubular Pipe (Venturi)	10 ± 1.3
3C: AquaB In-line Tubular Pipe (Air Comp.)	14 ± 1.6
4V: AquaB Radial Vortex (Venturi)	16 ± 2.1
4C: AquaB Radial Vortex (Air Comp.)	20 ± 2.4
5: Anzai Porous Membrane	2.1 ± 0.30
3V: AquaB In-line (Off-Grid, incl. P-drop)	8.6 ± 1.2

It can be readily seen that the NB-dissipation kinetics are a good deal more sluggish for electric-field-produced NBs, owing in part to the more dense electric-field NBs and build-up of gas molecules at the liquid interface [10].

Turning to submersible NB generators, the AquaB generator (7) was powered by mains electricity for AC–DC, and the Acniti microStar (6) was placed above the water line, and 10 lpm (STP) of air was added via a low-power air pump (~15 W). Important results are summarised in Table 8.

Table 8. NB populations ($\times 10^6$ NBs per mL) and power from air-fed submersible NB generators sampled after 20 min of operation in 20 litres; the number of asterisks details the number of successful NB measurements from three separate samples. The number of asterisks shows the number of successful detections of nanobubbles out of three attempts.

Type	Zetasizer	Nanosight	Power (W)	O_2—NBs (mg/L)	DO Boost (mg/L)	τ (days)
6: Acniti	3.15 ** $\pm$ 0.82	2.81 ** $\pm$ 0.64	15 + 400 = 415	0.12 ± 0.016	0.31 ± 0.03	1.8 ± 0.25
7: AquaB	34.7 *** $\pm$ 6.9	26.1 *** $\pm$ 4.0	15 + 5 = 20	1.3 ± 0.11	0.52 ± 0.06	9 ± 1.6

It is clear that the level of NB production, in terms of mass of NBs per unit power, is roughly ~10 × 20 = 200-times better for the electric-field approach, with about two-thirds of

the total DO being in NB form (as opposed to about a quarter for the Acniti case). Although the submersible type of electric-field NB generation, with no forced water convection, does not match the absolute performance of its water-flow electric-field counterpart in terms of NB mass concentration, the more passive nature of quiescent NB generation and NB propagation throughout the water body via natural convection currents is clearly a very attractive "passive" NB-generation approach. The longer-lived nature of air NBs generated via the electric-field approach compared to hammermill rotation (with a relaxation time some five-times longer at 9 versus 1.8 days, cf. Table 8) is also a desideratum for long-lived and passive air-fed nano-oxygenation. Similar results were witnessed for nanocarbonation in this same AquaB-versus-Acniti submersible comparison [31].

Clearly, this type of more passive NB-generation approach is of interest to water-body aeration/gasification in outdoor settings, whether in environmental water bodies or in aeration/carbonation tanks. Although the current study has, so far, been focused on clean-water "proof-of-concept" studies in indoor laboratory settings, having determined the essential superiority of the electric-field NB-generation approach (including, vitally, from an energy-efficiency perspective), in Figure S1 some "real-world" outdoor lake-based nanobubble-aeration results are presented for the suppression of a previous blight of cyanobacteria (cf. Supplementary Materials). It is striking that just a week was needed with 60 lpm air-pump flow (STP) at a discharge pressure of ~1 bar g to eradicate cyanobacteria and suppress eutrophication, as well as improve the health of the reeds and general aquatic health of carp fish. The DO was boosted by ~1.1 mg/L, whilst the ORP was increased by ~30 mV.

5. Conclusions

Industrially relevant and state-of-the-art "nanobubble-engineering" metrics have been measured for a variety of commercial NB generators to a level of scientific and instrumental rigour applied very rarely—at least regarding what has been published in the open scientific literature. Although the water-flow NB generators were run in recirculation mode for 4 min, further work can certainly be conducted in single-pass mode to study "virgin" NB generation only. Given that the Stokes' Law "buoyancy lifetime" of NBs is expected to be much longer than their own internal (meta)stability [1–3,9], the establishment of NB decay dynamics is particularly important—which the present study has accomplished.

In any event, it was found that the electric-field approach to NB generation surpasses traditional mechanical approaches for clean-water NB generation, especially when considering the energy running cost. In particular, more passive electric-field approaches are very operationally attractive for NB generation, where water and gas flow can be handled at little to no cost to the end operator, and/or submersible NB generators can be deployed, allowing for the use of photovoltaic approaches (with backup batteries for night-time and "low-sun" scenarios and air-/CO_2-pumping paraphernalia).

Electric-field approaches are expected to be even greater in superiority to mechanical-generation approaches for wastewater treatment, where porous-membrane blockages become an insurmountable problem—never mind the impractically high operating energy cost.

The present study has also called into question the level of bubble generation that is actually on the nanoscale in mechanically based commercially available generators that putatively produce NBs [42]. It has also sought to challenge the oft-prevailing industrial mindset of the (traditionally) dissolved gas level being characteristic of the effectiveness, or otherwise, of NB generation. Other metrics in water following fine-bubble generation, such as ORP and the relaxation thereof, or the time-resolved trajectory of DO (as opposed to the absolute value thereof in the immediate aftermath of fine-bubble generation) are more relevant to (putative) NB generation per se: hydrodynamically effective macrobubble generation can, and does, boost dissolved gas levels temporarily, for periods of tens of minutes until Stokes' Law dissipation (and/or chemical/biological gas demand) serves to reduce that. Therefore, actual and would-be NB-generator operators would do well to take

note of these "cautionary tales" in their operational assessment of the effectiveness of their nano-/fine-bubble-generation activities.

Supplementary Materials: The following supporting information can be downloaded at: https://www.mdpi.com/article/10.3390/app14177636/s1, Figure S1: (**a**) Photovoltaic-powered submersible AquaB NB generator on a float with a battery and DC-fed air pump at ~60 lpm air (STP); (**b**) ~2500 m^3 of cyanobacteria-laden water in a 1.5 m-deep lake at average temperatures of 27–35 deg C, with mid-afternoon phycocyanin Relative Fluorescence Unit (RFU) levels of 30–40, before an AquaB submersible unit was deployed, with shore-based solar (and battery) or mains electricity as an option, as well as "floating PV" (FPV) as in panel a; (**c**) Cyanobacteria eradication and suppression of eutrophication in the formerly benthic zone 7 days later.

Funding: This research was funded by European Innovation Council, No. 190166658.

Institutional Review Board Statement: Not applicable.

Informed Consent Statement: Not applicable.

Data Availability Statement: The original contributions presented in the study are included in the article/Supplementary Materials, further inquiries can be directed to the corresponding author.

Conflicts of Interest: The author declares no conflict of interest.

References

1. Kyzas, G.Z.; Mitropoulos, A.C. From bubbles to nanobubbles. *Nanomater* **2021**, *11*, 2592. [CrossRef] [PubMed]
2. Zhou, L.; Wang, S.; Zhang, L.; Hu, J. Generation and stability of bulk nanobubbles: A review and perspective. *Curr. Opin. Coll. Inter. Sci.* **2021**, *53*, 101439. [CrossRef]
3. Foudas, A.W.; Kosheleva, R.I.; Favvas, E.P.; Kostoglou, M.; Mitropoulos, A.C.; Kyzas, G.Z. Fundamentals and applications of nanobubbles: A review. *Chem. Eng. Res. Design* **2023**, *189*, 64–86. [CrossRef]
4. Sakr, M.; Mohamed, M.M.; Maraq, M.A.; Hamouda, M.A.; Hassan, A.A.; Ali, J.; Jung, J. A critical review of the recent developments in micro–nano bubbles applications for domestic and industrial wastewater treatment. *Alex. Eng. J.* **2022**, *61*, 6591–6612. [CrossRef]
5. Li, D.; Jing, D.; Pan, Y.; Bhushan, B.; Zhao, X. Study of the Relationship between Boundary Slip and Nanobubbles on a Smooth Hydrophobic Surface. *Langmuir* **2016**, *32*, 11287–11294. [CrossRef]
6. Wu, J.; Zhang, K.; Cen, C.; Wu, X.; Mao, R.; Zheng, Y. Role of bulk nanobubbles in removing organic pollutants in wastewater treatment. *AMB Express* **2021**, *11*, 96. [CrossRef]
7. Schubert, H. Nanobubbles, hydrophobic effect, heterocoagulation and hydrodynamics in flotation. *Inter. J. Mineral Proc.* **2005**, *78*, 11–21. [CrossRef]
8. Jin, J.; Yang, L.; Chen, F.; Gu, N. Drug delivery system based on nanobubbles. *Interdiscip. Mater.* **2022**, *1*, 471–494. [CrossRef]
9. Chen, E.; Zhang, Y.; Lu, S.; Duan, H.; Jin, W. Stability and physicochemical properties of air nanobubbles. *Chem. Ind. Eng. Prog.* **2022**, *41*, 4673–4681.
10. Ghaani, M.R.; English, N.J. Developments of Cutting-Edge Techniques for Facile Gas/liquid Nano-Bubble/Droplet Formation for Greatly-Enhanced Gas Storage in Liquids for Months (Several-Fold above Equilibrium Solubility), and Facile de-Gassing, British Patent Office, Oct. 2018. Ref. # 1816766.8, and Three Ensuing PCT Filings Now at National-Examination Stage in EU, Japan, USA, Canada, S. Korea, Saudi Arabia, China, Australia, New Zealand. These Three PCT Details Are as Follows: (i) A System, Method and Generator for Generating Nanobubbles or Nanodroplets PCT/EP2019/078003 (Oct 2019); (ii) A System and Method for the Treatment of Biogas and Wastewater PCT/EP/2019/078017 (Oct 2019); (iii) A System, Method and Generator for Generating Nanobubbles or Nanodroplets at Ambient Conditions PCT/EP2020/061107 (Apr 2020).
11. Ghaani, M.R.; Kusalik, P.G.; English, N.J. Massive generation of metastable bulk nanobubbles in water by external electric fields. *Sci. Adv.* **2020**, *6*, aaz0094. [CrossRef] [PubMed]
12. Sun, L.; Zhang, F.; Guo, X.; Qiao, Z.; Zhu, Y.; Jin, N.; Cui, Y.; Yang, W. Research progress on bulk nanobubbles. *Particuology* **2022**, *60*, 99–106. [CrossRef]
13. Meegoda, J.N.; Hewage, S.A.; Batagoda, J.H. Stability of Nanobubbles. *Environ. Eng. Sci.* **2018**, *35*, 1216–1227. [CrossRef]
14. English, N.J. Sustainable Exploitation and Commercialisation of Ultradense Nanobubbles: Reinventing Liquidity. *ACS Sust. Chem. Eng.* **2022**, *10*, 3383–3386. [CrossRef]
15. "Nanobubbles Provide a Pathway to Sustainability"—News Report and Interview with N.J. English in Chem. Eng. Prog. of AIChE-February 2023 Issue. Available online: https://www.aiche.org/resources/publications/cep/2023/february/cep-news-update/nanobubbles-provide-pathway-sustainability (accessed on 25 August 2024).
16. English, N.J. Electric-Field Nanobubbles for Agriculture. Open Access Government July 2024. pp. 388–389. Available online: https://www.openaccessgovernment.org/article/electric-field-nanobubbles-for-agriculture/178119/ (accessed on 25 August 2024).

17. English, N.J. Electric-Field Nanobubbles: Re-Engineering Water Treatment. Open Access Government April 2024. pp. 376–377. Available online: https://www.openaccessgovernment.org/article/electric-field-nanobubbles-re-engineering-water-treatment/175035/ (accessed on 25 August 2024).
18. English, N.J. Environmental Exploration of Ultra-Dense Nanobubbles: Rethinking Sustainability. *Environments* **2022**, *9*, 33. [CrossRef]
19. Jannesari, M.; Caslin, A.; English, N.J. Electric field-based air nanobubbles (EF-ANBs) irrigation on efficient crop cultivation with reduced fertilizer dependency. *J. Environ. Manage.* **2024**, *362*, 121228. [CrossRef] [PubMed]
20. Pan, M.; Naeiji, P.; English, N.J. Fate of Nanobubbles Generated from CO_2–Hydrate Dissociation: Coexistence with Nanodroplets—A Combined Investigation from Experiment and Molecular Dynamics Simulations. *Small Struct.* 2024; *early view*. [CrossRef]
21. Satoshi, A. Ultrafine Bubble Generation Device for Aquaculture or Wastewater Treatment. U.S. Patent Application 16/309653, 29 August 2019.
22. Yano, H.; Sakai, A. System and Method for Generating Nanobubbles. U.S. Patent Application 14/240,037, 10 July 2014.
23. Russell, W.S.; Scholten, B. Compositions Containing Nano-Bubbles in a Liquid Carrier. U.S. Patent 10598447, 6 September 2019.
24. Sang, Y.U.N. Device for Producing Nano-Bubble Water. ENH KOREA CO LTD OP-KR 20170118808 A, 2 November 2019.
25. Toshihiko, E. Floatation Separation Method of Particles in Liquid, and Apparatus Therefor. AURA TEC KK OP-JP 2008207226 A, 4 October 2010.
26. Shuhei, O.; Hitomi, T. Fine Bubble Generator and Method for Generation of the Same. YBM CO LTD OP-JP 2014161782 A, 6 August 2016.
27. Ho, Y.O.O.Y.; Geun, Y.O.O.T.A.E.; Ram, Y.O.O.A.H. Nano-Bubble Producing System Using Frictional Force. YOO YOUNG HO OP-KR 20190126340 A, 5 April 2020.
28. Ho, Y.O.O.Y.; Geun, Y.O.O.T.A.E.; Ram, Y.O.O.A.H. Flow Channel Member for Micro and/or Nano Bubble Integrated Flow Unit and Producing Device for Micro and/or Nano Bubble Using the Same. YOO YOUNG HO OP-KR 20190064273 A, 18 July 2020.
29. Scholten, B.; Shinde, P.M. Submersible Nano-Bubble Generating Device and Method. U.S. Patent 11331633, 13 March 2020.
30. Saremi, O.; Tuite, D.; English, N.J. Long-Time Water Aeration by Electrostriction-Generated Nanobubbles. *AIP Conf. Proc.* **2024**, *3084*, 050002.
31. Sangaru, S.; Abdel-Fattah, A.; English, N.J. Water Nano-Carbonation by CO_2 Infusion into Submersible and Pipe-Flow Nanobubble Generators: The Rise and Fall of Dissolved CO_2. *AIP Conf. Proc.* **2024**, *3084*, 050005.
32. Pan, M.; English, N.J. Dynamic Evolution of Metastable CO_2 Nanobubbles Generated by an External Electric Field. *AIP Conf. Proc.* **2024**, *3084*, 050003.
33. English, N.J. Enhancement of Calorific Performance of Internal Combustion Engines by Air Nanobubbles in Petroleum. *AIP Conf. Proc.* **2024**, *3084*, 050004.
34. Available online: https://www.moleaer.com/products/kingfisher (accessed on 25 August 2024).
35. Available online: https://www.acniti.com/products/turbiti-nano-bubble-mixer/ (accessed on 25 August 2024).
36. Available online: http://aqua-bubble.com/products/ (accessed on 25 August 2024).
37. Available online: https://anzaimcs.com/en/main/examplenanobubble.html (accessed on 25 August 2024).
38. Available online: https://www.acniti.com/products/microstar-ozone/microstar-fs400ac-1-specs/ (accessed on 25 August 2024).
39. English, N.J.; (Malvern Panalytical, Malvern, UK). Personal communication, 2023.
40. English, N.J.; (Particular Sciences, Dublin, Ireland). Personal communication, 2024.
41. Gao, S.; Zhong, C.; Wang, Z. A model describing the pressure drops across the membrane and cake layers for constant flux cross-flow microfiltration process. *J. Environ. Chem. Eng.* **2022**, *10*, 107984. [CrossRef]
42. Alheshibri, M.; Qian, J.; Jehannin, M.; Craig, V.S.J. A history of Nanobubbles. *Langmuir* **2016**, *32*, 11086–11100. [CrossRef] [PubMed]